Farnesylation of Nonpeptidic Thiol Compounds by Protein Farnesyltransferase[†]

Kendra E. Hightower,[‡,§] Patrick J. Casey,[‡,§] and Carol A. Fierke*[,‡,||]

Departments of Biochemistry and of Pharmacology and Cancer Biology, Duke University Medical Center, Durham, North Carolina 27710

Received September 22, 2000; Revised Manuscript Received November 14, 2000

ABSTRACT: Protein farnesyltransferase catalyzes the modification of protein substrates containing specific carboxyl-terminal Ca_1a_2X motifs with a 15-carbon farnesyl group. The thioether linkage is formed between the cysteine of the Ca_1a_2X motif and C1 of the farnesyl group. Protein substrate specificity is essential to the function of the enzyme and has been exploited to find enzyme-specific inhibitors for antitumor therapies. In this work, we investigate the thiol substrate specificity of protein farnesyltransferase by demonstrating that a variety of nonpeptidic thiol compounds, including glutathione and dithiothreitol, are substrates. However, the binding energy of these thiols is decreased 4−6 kcal/mol compared to a peptide derived from the carboxyl terminus of H-Ras. Furthermore, for these thiol substrates, both the farnesylation rate constant and the apparent magnesium affinity decrease significantly. Surprisingly, no correlation is observed between the pH-independent log(k_{max}) and the thiol pK_a; model nucleophilic reactions of thiols display a Brønsted correlation of approximately 0.4. These data demonstrate that zinc−sulfur coordination is a primary criterion for classification as a FTase substrate, but other interactions between the peptide and the FTase•isoprenoid complex provide significant enhancement of binding and catalysis. Finally, these results suggest that the mechanism of FTase provides in vivo selectivity for the farnesylation of protein substrates even in the presence of high concentrations of intracellular thiols.

Protein prenyltransferases catalyze the posttranslational lipid modification of one or more cysteine residues near the carboxyl terminus of proteins involved in signal transduction and membrane trafficking. A thioether linkage is formed between the cysteine sulfur and the isoprenoid group, either a 15-carbon farnesyl or a 20-carbon geranylgeranyl, of prenyl diphosphates (*1*, *2*). For the modified proteins, the prenyl groups serve as membrane anchors and may act as sites for protein−protein interactions (*1*, *3*). Attachment of the prenyl group(s) is required for the biological function of these proteins.

All three protein prenyltransferases, protein farnesyltransferase (FTase),[1] protein geranylgeranyltransferase type-I (GGTase-I), and protein geranylgeranyltransferase type-II (GGTase-II, also called RabGGTase), are heterodimeric zinc metalloenzymes (*1*, *4*). Crystal structures of FTase (*5*−*9*) and GGTase-II (*10*) show significant structural similarity, even though specific differences in the structures, thought to be related to substrate specificity and enzyme function, exist. The general catalytic mechanisms of the three protein prenyltransferases are likely to be similar, with the zinc ion being involved in catalysis and the diphosphate activated as a leaving group. The zinc ion coordinates the sulfur of the protein substrate Ca_1a_2X motif (*5*, *6*, *11*, *12*), thereby lowering the pK_a of the thiol so that a partially charged zinc thiolate can participate as a nucleophile in the reaction (*12*−*15*). A partial positive charge at C1 of the farnesyl or geranylgeranyl group contributes electrophilic character to the transition state (*14*, *16*). Formation of the positive charge at C1 is facilitated by activation of the diphosphate leaving group due to magnesium binding and/or interactions with residues in the active site (*15*, *17*).

Mutant forms of Ras have been implicated in up to 30% of all human cancers (*18*, *19*), and membrane targeting via the farnesyl group is necessary for the transformation of normal cells into cancerous cells by oncogenic forms of Ras (*20*−*22*). The substrate specificity of the protein prenyltransferases has been exploited to make FTase-specific inhibitors to serve as cancer chemotherapeutics (*23*−*25*), and several such compounds are currently in clinical trials (*26*). The specificity of protein prenyltransferases is determined primarily by the carboxyl-terminal sequence of the protein substrate: GGTase-II modifies both cysteine residues in

[†] This work was supported by National Institutes of Health Grants GM40602 (C.A.F.) and GM46372 (P.J.C.) and by the Cancer Research Fund of Damon Runyon−Walter Winchel Foundation Fellowship DRG-1450 (K.E.H.).

* To whom correspondence should be addressed.

[‡] Department of Biochemistry.

[§] Department of Pharmacology and Cancer Biology.

[||] Present address: Department of Chemistry, University of Michigan, 930 N. University, Ann Arbor, MI 48109-1055. Phone: (734) 936-2678. Fax: (734) 647-4865. E-mail: fierke@umich.edu.

[1] Abbreviations: FTase, protein farnesyltransferase; GGTase-I, protein geranylgeranyltransferase type-I; GGTase-II, protein geranylgeranyltransferase type-II; Hepes, *N*-(2-hydroxyethyl)piperazine-*N*′-2-ethanesulfonic acid; Heppso, *N*-(2-hydroxyethyl)piperazine-*N*′-2-hydroxypropanesulfonic acid; TCEP, tris(2-carboxyethyl)phosphine hydrochloride; FPP, farnesyl diphosphate; FMP, farnesyl monophosphate; [^{3}H]FOH, tritium-labeled farnesol; [^{3}H]FPP, tritium-labeled farnesyl diphosphate; FOH, farnesol; MTG, methyl thioglycolate; MG, methyl glycolate; bME, 2-mercaptoethanol; GSH, reduced glutathione; NAC, *N*-acetyl-L-cysteine; DTT, D/L-dithiothreitol; Bicine, *N*,*N*-bis(2-hydroxyethyl)glycine; I_{ana}, (*E*,*E*)-2-[2-oxo-2-[[(3,7,11-trimethyl-2,6,10-dodecatrienyl)oxy]amino]ethyl]phosphonic acid; GCVLS, pentapeptide Gly-Cys-Val-Leu-Ser; TLC, thin-layer chromatography.

10.1021/bi002237d CCC: $20.00
Published on Web 01/03/2001

motifs such as CC, CXC, or CCXX with geranylgeranyl groups while FTase and GGTase-I transfer a farnesyl and a geranylgeranyl group, respectively, to the cysteine residue in the Ca_1a_2X recognition motif (*1*). However, there is evidence that this peptide/protein specificity is not absolute. For example, several Ras proteins, including K-Ras and N-Ras, which are substrates for FTase can also be modified by GGTase-I (*27*−*30*) which may play a role in reducing the sensitivity of some cells to FTase inhibitors. In addition to protein and peptide substrates, FTase isolated from spinach has been reported to farnesylate dithiothreitol (*31*), a nonpeptidic thiol substrate. These findings suggest that: (1) FTase substrate specificity may not be as strict as previously surmised, (2) intracellular thiols may be substrates for FTase in vivo, and (3) FTase selectivity is likely tuned to ensure the farnesylation of protein substrates in vivo. Furthermore, these findings raise the question of whether thiol reducing agents commonly used during purification and biochemical characterization of protein prenyltransferases result in misleading kinetic parameters.

In this work, we investigate the ability of FTase to catalyze farnesylation of nonpeptidic thiol compounds. We demonstrate that a wide range of thiol compounds can be substrates for FTase with significant turnover numbers, even though both the binding affinity and the farnesylation rate constant are substantially reduced compared to a peptide substrate derived from the carboxyl terminus of H-Ras. In addition, partitioning studies indicate that, in contrast to peptide substrates, dissociation of the thiol compound from the FTase·FPP·RSH ternary complex is significantly faster than product formation. The kinetic characteristics of the reaction of FTase with the nonpeptidic thiol compounds suggest that this enzyme can efficiently and selectively farnesylate protein substrates even in the presence of high concentrations of intracellular thiol-containing compounds.

EXPERIMENTAL PROCEDURES

Preparation of FTase and Miscellaneous Procedures. Recombinant rat FTase was expressed in and purified from *Escherichia coli* as described previously (*32*) except that Hepes−NaOH (pH 7.7) was substituted for Tris-HCl. Before use, the enzyme was transferred into 50 mM Heppso−NaOH (pH 7.8), 1 mM tris(2-carboxyethyl)phosphine hydrochloride (TCEP), and 5 μM $ZnCl_2$ by dialysis. Enzyme concentrations were determined using a commercially available dye (Bio-Rad) in the Bradford assay (*33*). Peptides (HPLC-purified to ≥95%) were obtained from Applied Analytical Industries (Chapel Hill, NC). Peptide and thiol concentrations were determined by reaction of the cysteine with 5,5′-dithiobis-(2-nitrobenzoic acid) (*34*) using an extinction coefficient of 14 150 M^{-1} cm^{-1} (*35*) or by weight. Farnesyl diphosphate (FPP), farnesyl monophosphate (FMP), tritium-labeled FMP, and tritium-labeled farnesol ([^{3}H]FOH) were obtained from American Radiolabeled Chemicals, Inc. (St. Louis, MO). Tritium-labeled FPP ([^{3}H]FPP) was obtained from NEN LifeSciences (Boston, MA), and farnesol (FOH) was obtained from Kuraray Co. (Osaka, Japan). Methyl thioglycolate (MTG), methyl glycolate (MG), and 2-mercaptoethanol (bME) were obtained from Aldrich (Milwaukee, WI), reduced glutathione (GSH) and *N*-acetyl-L-cysteine (NAC) were obtained from Sigma (St. Louis, MO), and D/L-dithiothreitol (DTT) was obtained from VWR (West Chester, PA). All assays were conducted at 25 °C, and curve fitting was performed with KaleidaGraph (Synergy Software).

Thiol Binding Affinity. Dissociation constants for the thiols were measured with competition assays as described previously (*13*). The assays were performed in 50 mM buffer (Heppso−NaOH at pH 7.8, Bicine−NaOH at pH 9.1), ionic strength maintained at 0.1 M with NaCl, 5 mM TCEP, 5 mM $MgCl_2$, 0.01 μM EDTA, and 5% EtOH, with 0.02 μM FTase and 0.04 μM (*E,E*)-2-[2-oxo-2-[[(3,7,11-trimethyl-2,6,-10-dodecatrienyl)oxy]amino]ethyl]phosphonic acid (designated I_{ana}), an inactive isoprenoid analogue of FPP [(*36*); Calbiochem, San Diego, CA]. The Dns-GCVLS dissociation constant, K_D^{Dns}, was determined by direct titration of the peptide (excitation at 280 nm, emission at 496 nm) as described previously (*13*). For the competition assays, the thiols were titrated into a solution containing FTase, I_{ana}, and Dns-GCVLS at a concentration equal to K_D^{Dns}. The thiol dissociation constants, K_D^{RSH}, were calculated using eq 1:

$$FL = \frac{IF}{1 + (K_D^{Dns}/[Dns])(1 + [RSH]/K_D^{RSH})} + EP \quad (1)$$

where FL is the fluorescence of the bound Dns-GCVLS, IF is the initial fluorescence, EP is the fluorescence endpoint, [Dns] is the concentration of Dns-GCVLS, and [RSH] is the concentration of thiol.

Transient Kinetics. The FTase·[^{3}H]FPP binary complex was preformed by incubation of 0.75 μM FTase with 0.35 μM [^{3}H]FPP (20 Ci/mmol) in 50 mM Heppso−NaOH (pH 7.8), 20 mM TCEP, 5 mM $MgCl_2$, and 5% EtOH. The reaction (7.5 μL total volume) was initiated by the addition of thiol substrate (0.05−100 mM) and was stopped at various times (5 s to 4 h) by the addition of an equal volume of 2-propanol. The reactants and products were separated by thin-layer chromatography (TLC) on plastic-backed silica gel plates using a 6:3:1 or 8:1:1 (v/v/v) 2-propanol/NH_4OH/H_2O (GCVLS, NAC, and GSH) or a 70−80% MeOH (MTG, DTT, and bME) mobile phase. The tritium-labeled bands were visualized by autoradiography using an intensifying screen (TranScreen LE; Kodak, Rochester, NY) or following fluorographic enhancement (En^{3}Hance; NEN LifeSciences, Boston, MA). They were then excised, and the radioactivity was quantified by scintillation counting. The percentage of product formed represents the ratio of the radioactivity in the product band to the total radioactivity. The observed rate constant for product formation, k_{obs}, was calculated using eq 2:

$$\%P(t) = EP(1 - e^{-k_{obs}t}) \quad (2)$$

where $\%P(t)$ is the percentage of product at time t and EP is the percentage at the endpoint.

For the pH dependence study, the reactions were performed in 100 mM Bicine−NaOH (pH 7.8 or 9.1), total ionic strength maintained at 0.2 M with NaCl, 20 mM TCEP, 10 mM $MgCl_2$, and 5% EtOH, with 0.6 μM FTase, 0.25 μM [^{3}H]FPP (20 Ci/mmol), and 0.05−100 mM thiol. The assays and product analysis were performed as described above. The observed rate constant for product formation, k_{obs}, was determined by fitting eq 2 to the time-dependent product formation for the individual thiol concentrations. The maximal rate constant for product formation at saturating

thiol concentrations, k_{max}, and the thiol concentration at half-k_{max}, $K_{1/2}$, were calculated using eq 3:

$$k_{obs} = \frac{k_{max}}{1 + (K_{1/2}/[RSH])} \quad (3)$$

For the magnesium dependence study, the reactions were performed in 50 mM Heppso−NaOH (pH 7.8), 20 mM TCEP, 5% EtOH, and 1−120 mM $MgCl_2$, with 0.75 μM FTase, 0.35 μM [^{3}H]FPP (20 Ci/mmol), and 40 mM thiol. The ionic strength due to added salt was maintained at 0.36 M with NaCl. The assays and product analysis were performed as described above. The maximal rate constant for product formation at saturating magnesium concentrations, k_{max}^{Mg}, and the magnesium concentration at half-k_{max}^{Mg}, $K_{1/2}^{Mg}$, were calculated using eq 3 with the concentration of magnesium replacing the concentration of thiol.

Partitioning. The partitioning experiments were performed in 50 mM Heppso−NaOH (pH 7.8), 20 mM TCEP, 5 mM $MgCl_2$, and 5% EtOH, with 0.75 μM FTase, 0.35 μM [^{3}H]-FPP (20 Ci/mmol), and 40 mM thiol (7.5 μL total volume). The reactions were initiated by the addition of thiol to the FTase·[^{3}H]FPP binary complex and were allowed to incubate for 2−6 min so that 20−30% of the [^{3}H]FPP was converted to farnesyl-thiol. The reactions were then either quenched with an equal volume of 2-propanol or 30 μM GCVLS was added and incubated for 10 s before quenching. The assay components were separated by TLC using an 8:1:1 (v/v/v) 2-propanol/NH_4OH/H_2O mobile phase, and product analysis was performed as described above.

Steady-State Kinetics. Steady-state assays were performed in 50 mM Heppso−NaOH (pH 7.8), 20 mM TCEP, 5 mM $MgCl_2$, and 5% EtOH, or in 100 mM Bicine−NaOH (pH 7.8), total ionic strength maintained at 0.2 M with NaCl, 20 mM TCEP, 10 mM $MgCl_2$, and 5% EtOH, with saturating [^{3}H]FPP (2−4 μM, 2.6 Ci/mmol) and varied thiol substrate (0.025−10 μM GCVLS or 0.45−80 mM thiol). The assays were initiated by the addition of FTase, 1−5 nM for the GCVLS reactions or 50 nM for the thiol reactions. The reactions were stopped at various times (15 s to 6 h) by the addition of an equal volume of 2-propanol so that less than 10% product was formed based on limiting substrate concentration. Product formation was quantified by TLC and scintillation counting as described above. The steady-state parameters k_{cat} and K_m were calculated using eq 4:

$$\frac{v}{[E]_{tot}} = \frac{k_{cat}[S]}{[S] + K_m} \quad (4)$$

or k_{cat} was calculated from the initial velocity of the reaction at saturating substrate concentrations.

Synthesis of Farnesylated Standards. Farnesyl-MTG and farnesyl-bME were synthesized by reacting farnesyl bromide (0.58 mmol) and the thiol compound (0.58 mmol) for 1.5 h on ice with stirring in a solution containing 1.75 mmol of zinc acetate in 4.5 mL of 2:1:1 (v/v/v) dimethylformamide/acetonitrile/0.025% trifluoroacetic acid (*37*, *38*). The solutions were loaded onto preparative silica gel TLC plates containing a fluorescent indicator (excitation at 254 nm), and the plates were developed in 90% 2-propanol. The top band, corresponding to the fluorescence quenching, was removed, and the silica was extracted with 2:1 (v/v) chloroform/MeOH. The solutions were dried, and the resulting powders were resuspended in 2-propanol. The identities of the farnesyl-MTG and farnesyl-bME standards were confirmed by the Mass Spectrometry Facility at Duke University.

RESULTS

Alternate Thiol Substrates. Modified proteins and short peptides that mimic the Ca_1a_2X motif have been extensively used to study the substrate specificity of FTase (*39*−*44*). These studies showed that both the sequence of the Ca_1a_2X motif and the positioning of the cysteine as the fourth residue from the carboxyl terminus are important criteria for classification of a peptide/protein as an FTase substrate. However, several reports have suggested that the apparent peptide/protein substrate specificity can be variable (*27*−*31*, *45*−*48*). These conclusions were primarily based on steady-state kinetic parameters (k_{cat}, K_m, and k_{cat}/K_m) or on the ability of the peptide to inhibit farnesylation of protein substrates. For mammalian FTase, steady-state parameters do not necessarily reflect the thermodynamic affinity of FTase substrates since peptide and product dissociation are significantly slower than the chemical step (*11*, *14*, *49*−*52*). To determine the minimal requirements for substrate recognition and utilization by FTase, we chose to examine the ability of FTase to catalyze farnesylation of a number of nonpeptidic thiol compounds (Figure 1). Except for the free thiol group(s), these compounds bear little resemblance to the peptide, GCVLS, derived from the carboxyl terminus of H-Ras (KCVLS), that has previously been used to study the catalytic mechanism of FTase (*13*−*15*, *51*).

Binding to FTase. To determine if FTase could bind the thiol compounds, a fluorescence-based competition assay (*13*) was used to measure the affinity of a binary complex, comprised of FTase and an inactive isoprenoid phosphonate designated I_{ana} (Figure 1), for the compounds. The thiol compounds compete with Dns-GCVLS for binding to FTase·I_{ana}, as indicated by a decrease in fluorescence, demonstrating that they bind in the peptide binding pocket (Figure 2). The nonthiol analogue of MTG, MG (Figure 1), does not compete with Dns-GCVLS for binding to the FTase·I_{ana} binary complex even at concentrations greater than 1 mM. The affinity of the FTase·I_{ana} binary complex for the thiol compounds is significantly weaker, at least 400-fold (Table 1), than the affinity for the peptide GCVLS. The relatively high affinity for DTT compared to the other thiols may be due to bidentate metal coordination of both sulfur atoms of DTT. The observed decreases in K_D for the thiols relative to the peptide demonstrate that the zinc−sulfur coordination is not sufficient to achieve the high-affinity binding observed for peptide and protein substrates (*13*). Therefore, other favorable interactions between the peptide and the enzyme−isoprenoid complex provide a significant portion of the binding energy. Interactions between the enzyme and Ca_1a_2X peptide substrates that could be energetically important, including hydrogen bonds with Arg202β and Gln167α, have been visualized in crystal structures of ternary complexes (*5*, *6*).

Product Formation with Thiols. To determine if FTase can use nonpeptidic thiol compounds as substrates, the thiol compounds were incubated with a FTase·[^{3}H]FPP binary complex. A tritium-labeled product is formed for each thiol,

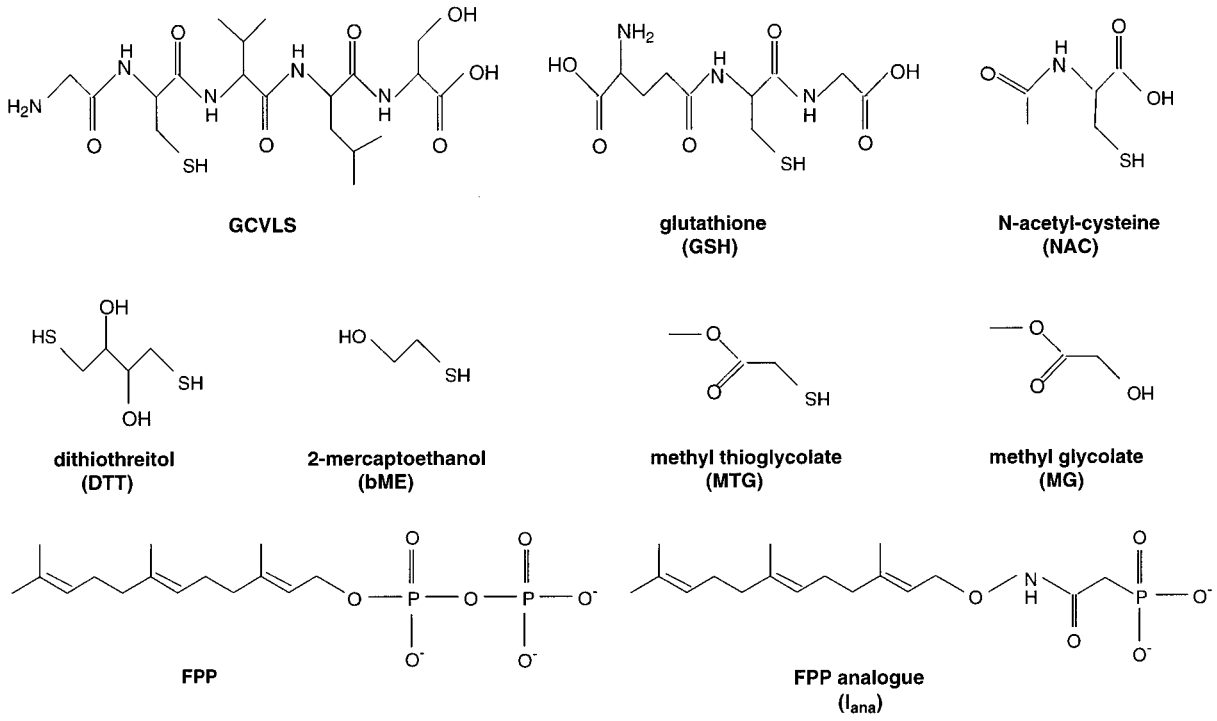

FIGURE 1: Structures of substrates and analogues.

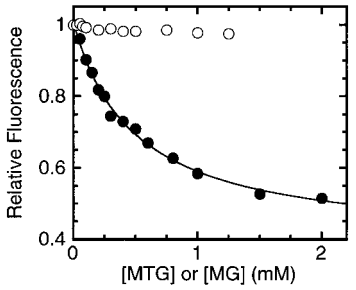

FIGURE 2: Competition with peptide for binding. The binding affinity of an FTase·I_{ana} binary complex for compounds was determined by competition with Dns-GCVLS in 50 mM Heppso−NaOH (pH 7.8), ionic strength maintained at 0.1 M with NaCl, 5 mM TCEP, 5 mM $MgCl_2$, 0.01 μM EDTA, and 5% EtOH. MTG (●) or MG (○) was titrated into a solution containing 0.02 μM FTase, 0.04 μM I_{ana}, and 0.08 μM Dns-GCVLS. The data shown are relative to the initial fluorescence values of 3.3 and 2.8 for MTG and MG, respectively.

as indicated by TLC on silica gel plates. Since the tritium label on the [^{3}H]FPP is at the C1 position of the farnesyl chain, the tritium-labeled products have incorporated the farnesyl group. The farnesylated products migrate distinctly from each other and from FPP, FMP, and FOH on TLC plates and by HPLC analysis (Table 2). The farnesylated products of the reaction of FTase·FPP with MTG and bME comigrate with chemically synthesized farnesyl-MTG and farnesyl-bME, respectively, both on TLC plates containing a fluorescent indicator (data not shown) and on a C18 reverse phase HPLC column (Table 2). These results indicate that the farnesylated products of the reactions of FTase·FPP with the thiol compounds are the farnesyl-thiols. The thiol group is required for formation of the farnesylated product; product formation was not observed with MG, the nonthiol analogue of MTG.

Transient Kinetics. To compare the efficiency of FTase-catalyzed farnesylation of nonpeptidic substrates to peptide substrates, both transient and steady-state kinetic analyses were performed. For the transient kinetic studies, single-turnover reactions with saturating enzyme concentration relative to the limiting FPP substrate were used to measure the observed rate constant for product formation, k_{obs} (see Scheme 1). The single-turnover reactions proceed to completion, and the data are well-described by a single first-order exponential (Figure 3A, eq 2). We then measured the dependence of this observed rate constant on the concentration of thiol. In all cases, a single exponential fits well to the data, and the concentration dependence of the rate constant could be described by saturation of the FTase·FPP complex to form FTase·FPP·RSH (Figure 3B, eq 3). Although these nonpeptidic thiols are substrates, the single-turnover rate constants at saturating thiol and enzyme concentrations, k_{max} (Table 1), are reduced more than 10^3-fold compared to k_{max} for the peptide substrate GCVLS (*14*, *15*). Furthermore, the concentration of substrate at the half-maximal rate constant, $K_{1/2}$, ranged from 1.5 to 9.6 mM at pH 7.8 (Table 1), which is more than 75-fold larger than the value of 0.02 mM measured for GCVLS (*14*). These data demonstrate that, while FTase can catalyze farnesylation of a wide variety of thiol compounds, interactions between the protein and the peptide substrate in addition to the zinc−sulfur coordination are essential for high-affinity binding and efficient catalysis.

Interestingly, for peptidic and nonpeptidic thiol substrates, the $K_{1/2}$ is significantly larger than the measured K_D (Table 1). For peptide substrates, this result is predicted from the kinetic mechanism. Since the rate constant for the chemical step is much greater than the rate constant for dissociation of the peptide ($k_2 \gg k_{-1}$ in Scheme 1), $K_{1/2}$ does not reflect K_D but rather reflects a change in the rate-limiting step from substrate binding to chemistry as the concentration of peptide increases (*11, 14, 49*). However, this explanation likely does not describe the nonpeptidic thiol data as both the chemical rate constant and the substrate affinity decrease significantly.

Table 1: pH Dependence of Kinetic Constants[a]

		pH 7.8			pH 9.1		
substrate	pK_a[b]	K_D (mM)	$K_{1/2}$ (mM)	k_{max} (s^{-1})	K_D (mM)	$K_{1/2}$ (mM)	k_{max} (s^{-1})
Dns-GCVLS	8.3	$(6.8 \pm 0.8) \times 10^{-5}$	ND	4.2[c]	$(2.6 \pm 0.5) \times 10^{-5}$	ND	ND
GCVLS	8.6	$(6.8 \pm 0.1) \times 10^{-5}$	0.02[c]	9.1[d]	ND	ND	10[d]
GSH	9.0	0.12 ± 0.01	9.6 ± 1.4	$(5.3 \pm 0.2) \times 10^{-3}$	0.062 ± 0.007	3.0 ± 0.2	$(1.5 \pm 0.03) \times 10^{-2}$
MTG	8.0	0.22 ± 0.06	8.1 ± 0.5	$(5.5 \pm 0.2) \times 10^{-3}$	0.28 ± 0.02	4.6 ± 0.2	$(6.9 \pm 0.2) \times 10^{-3}$
bME	9.4	0.82 ± 0.08	7.2 ± 0.2	$(1.6 \pm 0.05) \times 10^{-3}$	0.17 ± 0.01	1.0 ± 0.04	$(1.7 \pm 0.05) \times 10^{-3}$
NAC	9.5	0.20 ± 0.04	ND	$(2.2 \pm 0.2) \times 10^{-3}$	ND	ND	ND
DTT	9.1, 10.1	0.03 ± 0.0004	1.5 ± 0.3	$(1.9 \pm 0.4) \times 10^{-3}$	ND	ND	ND

[a] All assays were conducted at 25 °C. The K_D values were determined in 50 mM Heppso−NaOH (pH 7.8) or Bicine−NaOH (pH 9.1), ionic strength maintained at 0.1 M with NaCl, 5 mM TCEP, 5 mM $MgCl_2$, 0.1 μM EDTA, and 5% EtOH. The $K_{1/2}$ and k_{max} values for the thiols were determined in 100 mM Bicine−NaOH (pH 7.8 or 9.1), total ionic strength maintained at 0.2 M with NaCl, 20 mM TCEP, 10 mM $MgCl_2$, and 5% EtOH. ND denotes not determined. [b] The pK_a values were obtained from (*13*) for GCVLS and Dns-GCVLS, (*59*) for GSH, and (*67*) for MTG, bME, NAC, and DTT. [c] These values were obtained from (*14*). [d] These values were obtained from (*15*).

Table 2: Chromatographic Separation of Farnesyl-Containing Compounds

compound	R_f[a]	R_f[b]	retention time (min)[c]
FPP	0	0	32.7
FMP	−	0.77	34.5
FOH	0.87	0.8	43.6
F-bME	−	0.59	46.8 (46.9)
F-MTG	−	0.36	51.1 (51)
F-DTT	−	0.54	−
F-GCVLS	0.6	−	−
F-NAC	0.71	−	−
F-GSH	0.25	−	−

[a] Separated on a silica gel TLC plate with an 8:1:1 (v/v/v) 2-propanol/NH_4OH/H_2O mobile phase. [b] Separated on a silica gel TLC plate with a 75% MeOH mobile phase. [c] Separated on a reverse phase C18 column (250 × 4.6 mm, Phenomenex) with a gradient (55 min, 1 mL/min) of 10% acetonitrile, 0.1% trifluoroacetic acid to 100% acetonitrile, 0.1% trifluoroacetic acid. The values in parentheses are for the chemically synthesized products.

Scheme 1: General Reaction Scheme for Farnesylation of Thiols[a]

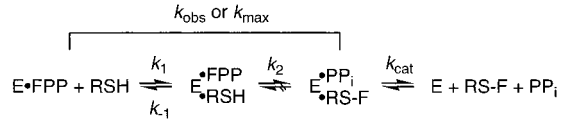

[a] In this scheme, E is protein farnesyltransferase, FPP is farnesyl diphosphate, RSH is a thiol compound, and RS−F is the farnesylated thioether product. The thiol association and dissociation rate constants are represented by k_1 and k_{-1}, respectively, and the rate constant for product formation (chemistry) is denoted by k_2. The steady-state rate constant k_{cat} represents rate-limiting product release for peptide and protein substrates. In the experiments presented here, k_{obs}, the observed rate constant for product formation, and k_{max}, the maximal rate constant for product formation, were measured at subsaturating and saturating thiol concentrations, respectively.

Furthermore, partitioning experiments (described below) demonstrate that the FTase•FPP•RSH ternary complex is in rapid equilibrium with free RSH. Therefore, the simplest explanation for the lower K_D compared to $K_{1/2}$ for the nonpeptidic thiols is that they bind more tightly to the FTase•I_{ana} complex used in the binding affinity experiments than they do to the catalytically competent FTase•FPP complex. An alternative explanation is that the chemical step is no longer rate-limiting in the reaction with the thiols, but rather that another step, such as a conformational change, becomes rate-limiting.

Partitioning. To determine if the ternary complex of FTase•FPP•RSH is formed rapidly and irreversibly, as

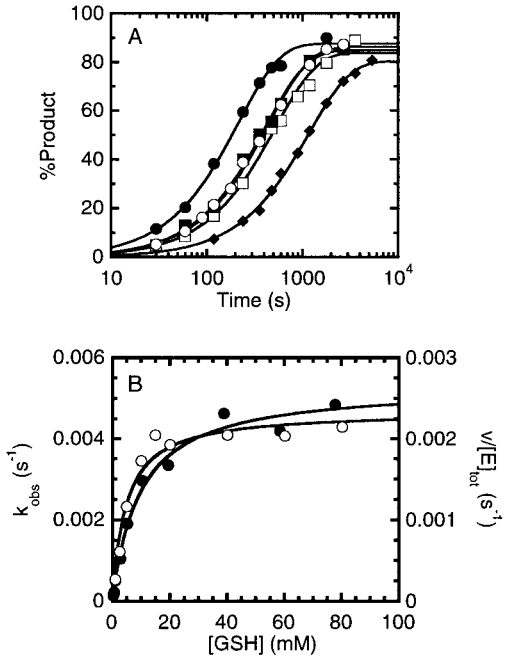

FIGURE 3: Time and concentration dependence of thiol farnesylation. (A) Time course for farnesylation of thiols. Single-turnover assays were conducted at 25 °C in 50 mM Heppso−NaOH (pH 7.8), 20 mM TCEP, 5 mM $MgCl_2$, and 5% EtOH with an FTase•[^{3}H]FPP binary complex (0.75 μM FTase, 0.35 μM [^{3}H]FPP) and 40 mM GSH (●), NAC (○), MTG (■), DTT (□), or bME (◆). The reactions were quenched by the addition of an equal volume of 2-propanol, and the %Product was determined by TLC and scintillation counting. Observed rate constants for product formation, k_{obs}, ranging from 0.8×10^{-3} s^{-1} (bME) to 4.5×10^{-3} s^{-1} (GSH), were obtained by fitting eq 2 to the individual time courses. (B) Concentration dependence of single-turnover and steady-state catalysis for GSH. Single-turnover (●) and steady-state (○) assays were conducted at 25 °C in 100 mM Bicine−NaOH (pH 7.8), total ionic strength maintained at 0.2 M with NaCl, 20 mM TCEP, 10 mM $MgCl_2$, and 5% EtOH as described under Experimental Procedures. The concentration dependence of the single-turnover reaction results in $K_{1/2} = 9.6 \pm 1.4$ mM and $k_{max} = (5.3 \pm 0.2) \times 10^{-3}$ s^{-1} (eq 3) while the concentration dependence of steady-state catalysis results in $K_m = 4.9 \pm 1.2$ mM and $k_{cat} = (2.4 \pm 0.2) \times 10^{-3}$ s^{-1} (eq 4).

observed for peptide substrates ($k_2 \gg k_{-1}$ in Scheme 1), pulse−chase experiments were performed. In these experiments, the FTase•[^{3}H]FPP•RSH complex is formed under saturating concentrations of RSH and FTase with limiting FPP and then mixed with the peptide GCVLS. Under these conditions, if product formation from the FTase•FPP•RSH complex is irreversible and faster than thiol dissociation (k_2

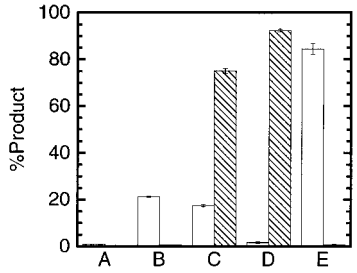

FIGURE 4: Partitioning with bME. The experiment was conducted at 25 °C with bME as described under Experimental Procedures. A, background without addition of either bME or GCVLS; B, 6 min reaction with bME; C, 6 min reaction with bME followed by addition of GCVLS for 10 s; D, 10 s reaction with GCVLS; E, 90 min reaction with bME. The open boxes represent farnesyl-bME, and the hatched boxes represent farnesyl-GCVLS.

$\gg k_{-1}$ in Scheme 1), only the farnesyl-thiol product will be observed despite the addition of peptide. However, if farnesylation is slow relative to substrate dissociation ($k_{-1} \gg k_2$), the added peptide substrate will bind to the FTase·FPP binary complex and react [$k_{obs} > 1\ s^{-1}$ (*11*, *14*, *15*)] to form the farnesyl-peptide. The results for partitioning experiments conducted with bME are shown in Figure 4. The reaction was initiated by the addition of 40 mM bME to an FTase·[^{3}H]FPP binary complex, allowed to react until 20−30% product was formed, and then the reaction was either quenched or diluted into peptide. After addition of GCVLS to the reaction, only the farnesyl-peptide product was observed with no additional farnesylation of bME. Similar results were obtained for GSH, NAC, DTT, and MTG (data not shown). These data demonstrate that the FTase·FPP·RSH complexes can react rapidly with peptide to form farnesyl-peptide, indicating that the rate constant for dissociation of thiol is rapid compared to farnesylation of bound thiol ($k_{-1} \gg k_2$) under these conditions. Therefore, the FTase·FPP·RSH complex should equilibrate rapidly and reversibly with the free thiol substrates under both steady-state and single-turnover conditions.

Steady-State Catalysis. The comparative reactivity of peptide and thiol substrates under steady-state conditions was also determined. For peptide and protein substrates, product release is rate-limiting under steady-state conditions with saturating substrate concentrations, so k_{cat} does not reflect the chemical step (*49*, *52*) (see Scheme 1). Consistent with this, k_{cat} for GCVLS, $0.18 \pm 0.06\ s^{-1}$ (Table 3), is approximately 70-fold lower than the maximal rate constant for product formation, k_{max} (Table 1). The k_{cat} value for GCVLS measured here is somewhat higher than previously reported values [$0.02-0.06\ s^{-1}$ (*14*, *51*)] due to the high concentration of TCEP which appears to accelerate the product dissociation rate constant (data not shown). FTase can also catalyze multiple turnovers with the thiol compounds, although the k_{cat} values for the thiol substrates are 130−420-fold lower than k_{cat} for GCVLS (Table 3). To directly compare the specificity of FTase for different thiol compounds, k_{cat}/K_m was determined for GCVLS, GSH, and MTG (Table 3). The k_{cat}/K_m values for MTG and GSH are decreased 5×10^4- and 2×10^5-fold, respectively, showing both that FTase is specific for peptide substrates and that these thiols are not efficient substrates for steady-state catalysis. For the thiol compounds, k_{max} and k_{cat} are comparable (within a factor of 3), suggesting that product release may not be entirely rate-limiting in steady-state turnover. Furthermore, the similarity between K_m and $K_{1/2}$ (within a factor of 2) would be consistent with a kinetic mechanism where the thiol substrate binds rapidly and reversibly followed by a rate-limiting step that is the same for k_{max} and k_{cat}.

Table 3: Steady-State Kinetic Data for Thiol Compounds[a]

substrate	k_{cat} (s^{-1})	K_m (mM)	k_{cat}/K_m ($mM^{-1}\ s^{-1}$)
GCVLS	0.15 ± 0.01[b]	0.0016 ± 0.0004	94
	0.18 ± 0.06		
GSH	$(2.4 \pm 0.2) \times 10^{-3}$ [b]	4.9 ± 1.2	0.00049
	$(1.4 \pm 0.2) \times 10^{-3}$		
MTG	$(9.6 \pm 0.4) \times 10^{-3}$ [b]	5.8 ± 1.0	0.0017
	$(3.4 \pm 0.2) \times 10^{-3}$		
bME	$(0.4 \pm 0.1) \times 10^{-3}$	ND	ND
NAC	$(1.3 \pm 0.2) \times 10^{-3}$	ND	ND
DTT	$(0.7 \pm 0.1) \times 10^{-3}$	ND	ND

[a] Unless otherwise indicated, the values were determined in 50 mM Heppso−NaOH (pH 7.8), 20 mM TCEP, 5 mM $MgCl_2$, and 5% EtOH at 25 °C with saturating substrate concentrations and represent averages of at least 3 separate experiments. [b] These values were determined at 25 °C in 100 mM Bicine−NaOH (pH 7.8), total ionic strength maintained at 0.2 M with NaCl, 20 mM TCEP, 10 mM $MgCl_2$, and 5% EtOH and result from fitting eq 4 to the data. ND denotes not determined.

pH Dependence. The reactivity and affinity of peptide substrates are dependent on the formation of the zinc-thiolate (*11*−*15*). To study the role of thiol ionization in binding and activity of the nonpeptidic thiol substrates, dissociation and single-turnover kinetic constants were determined at pH 9.1 for comparison with the data at pH 7.8. For each of the thiol compounds, the observed second-order rate constant for the reaction of total thiol with the FTase·FPP complex, $k_{max}/K_{1/2}$, increases with increasing pH. In fact, the increase in this observed rate constant correlates reasonably well with the increased concentration of the free thiolate, determined by the pK_a of the free thiol, as the pH increases to 9.1. For GSH and MTG, the rate increases are 11- and 2-fold, respectively, compared to calculated increases in the thiolate concentration of 9.4- and 2.4-fold at pH 9.1 compared to pH 7.8. These data suggest that the substrate thiolate is the reactive species, as observed for peptide substrates (*14*, *15*). However, this increase in reactivity is observed as both a decrease in $K_{1/2}$ and an increase in k_{max} as the pH increases. Furthermore, the thiol dissociation constant from the FTase·I_{ana}·RSH complex (K_D, Table 1) decreases at pH 9.1, paralleling the diminution in $K_{1/2}$. For peptides, pH dependence studies suggest that both the thiol and thiolate forms of the peptide can bind to the enzyme and that interaction of the sulfur with the zinc lowers the pK_a of the thiol by approximately 2 pH units (*12*, *13*, *15*). A similar model can explain the observed pH dependence for these thiol compounds. In fact, the pH dependence of k_{max} and $K_{1/2}$ can be quantitatively described using a pK_a for the thiol in the FTase·FPP·RSH complex of approximately 7.3 for MTG and 8 for bME and GSH using the equation $k_{max} = k_0/(1 + [H^+]/K_{a2})$. Therefore, binding of the thiol to the enzyme decreases the pK_a in each case by 1−2 pH units. However, no correlation between the pH-independent log(k_{max}) and pK_a is observed with these thiols. In model nucleophilic reactions of thiols, a plot of the pH-independent log(k_{obs}) versus pK_a of the thiol has a Brønsted correlation of approximately 0.4 (*53*−*59*). The lack of correlation in the enzyme reaction can be interpreted in

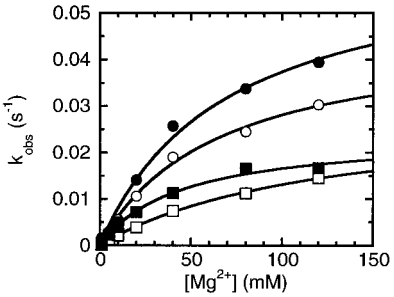

FIGURE 5: Magnesium dependence of thiol farnesylation. The observed rate constants for product formation, k_{obs} (eq 2), were determined at 25 °C for the reaction of FTase·[^{3}H]FPP (0.75 μM FTase, 0.35 μM [^{3}H]FPP) with 40 mM MTG (●), DTT (○), GSH (■), and bME (□) over a range of $MgCl_2$ concentrations (1−120 mM) in 50 mM Heppso−NaOH (pH 7.8), 20 mM TCEP, and 5% EtOH. The ionic strength due to added salt was maintained at 0.36 M with NaCl. The apparent k_{max}^{Mg} and $K_{1/2}^{Mg}$ values, respectively, are: 0.024 ± 0.002 s^{-1} and 45 ± 7 mM for GSH, 0.046 ± 0.003 s^{-1} and 65 ± 9 mM for DTT, 0.063 ± 0.007 s^{-1} and 68 ± 16 mM for MTG, and 0.029 ± 0.002 s^{-1} and 123 ± 12 mM for bME (eq 3 with [Mg^{2+}] replacing [RSH]).

several ways. One explanation is that there is no significant nucleophilic component in the transition state due to either significant dissociative character or a rate-limiting conformational change. Alternatively, the reactivity of these thiol compounds could be dominated by the positioning of the thiolate nucleophile relative to C1 of FPP rather than the reactivity of the nucleophile. In addition to the alterations in pK_a, the compounds examined in this study have significant structural differences (Figure 1) that could also lead to different reactivities.

Magnesium Dependence. In addition to the tightly bound zinc ion, millimolar concentrations of magnesium ions are required for efficient catalysis by FTase (*14, 15, 60*−*62*). Previous work has suggested that the magnesium ion enhances a step after formation of the ternary complex and at or before the chemical step (*14, 15*). In single-turnover reactions, the observed rate constant for farnesylation of peptides shows a hyperbolic dependence on the magnesium ion concentration. Furthermore, protonation of a group with a pK_a ∼ 7.4, proposed as a diphosphate hydroxyl in the ternary complex (*15*), increases the $K_{1/2}$ for magnesium, $K_{1/2}^{Mg}$, presumably by direct competition of the proton with a magnesium ion. A model consistent with these data is that at least one magnesium ion coordinates the diphosphate to stabilize the developing negative charge on the leaving group and to facilitate formation of a partial positive charge on C1 of FPP. Alternatively, the magnesium ion could stabilize a catalytically competent conformation of the FTase·FPP·peptide ternary complex. For GCVLS at pH 7.8, the apparent magnesium dissociation constant is 2 mM (*15*). Unexpectedly, the thiol compounds exhibit a greater dependence on the concentration of magnesium than the peptide substrate. The maximal rate constant for product formation with the thiol compounds is not achieved at 120 mM $MgCl_2$; fitting a binding isotherm to the data suggests that the $K_{1/2}^{Mg}$ varies from 45 mM for GSH to ∼120 mM for bME (Figure 5). Furthermore, at saturating magnesium concentrations, the observed rate constant for farnesylation is enhanced 10−25-fold compared to the rate constant at 5 mM magnesium. However, the farnesylation rate constant k_{max}^{Mg} is still several orders of magnitude slower than farnesylation of GCVLS. The dramatically increased magnesium dependence of the thiol reaction is not due to alteration of the pK_a of the diphosphate hydroxyl in the ternary complex since the magnesium dependence of the thiol reaction is unchanged at pH 9.1 (data not shown). Therefore, these data suggest that the magnesium affinity of the ternary complex is decreased with bound RSH compared to GCVLS, perhaps due to decreased affinity of the deprotonated diphosphate for magnesium. In crystal structures of binary and ternary complexes of FPP bound to FTase (*5*−*7*), a number of positively charged residues are observed that could potentially compete with magnesium for interaction with the diphosphate oxygens. This increased magnesium dependence of the enzyme with these thiol compounds may demonstrate another aspect of the synergism between the peptide substrate and prenyl substrate; binding of the peptide alters the interactions between FPP and the enzyme to enhance the magnesium affinity. Alternatively, the catalytic magnesium ion that activates the reactivity of these thiol substrates does not interact with the diphosphate oxygens but binds at an alternative position to activate the reaction.

DISCUSSION

Substrate Specificity and Catalytic Mechanism. We have demonstrated that FTase can catalyze the farnesylation of a variety of nonpeptidic thiol compounds. These results suggest that the presence of a free thiol is the primary criterion for classification as a FTase substrate. Indeed, the lack of a thiol (Ala or Ser substituted for Cys in CaaX, MG) or modification of the thiol results in the loss of binding affinity and of the ability to form product (*13, 20, 39, 41, 63*−*65*). As observed in optical absorbance spectra of FTase (*11, 12*) and structures of FTase·isoprenoid·peptide ternary complexes (*5, 6*), the sulfur of the substrate thiol interacts directly with the metal in the active site. Therefore, the zinc−sulfur interaction has been proposed as the most important interaction between the substrate and the enzyme. The zinc ion is required for catalysis and high-affinity peptide and protein, but not isoprenoid, binding (*14, 60, 66*). In addition, the modulation of the pK_a of the thiol due to interaction with the zinc, which results in a partially charged thiolate at physiological pH that can act as a nucleophile in the reaction, is an integral component of the catalytic mechanism (*12*−*15*). The zinc−sulfur interaction has also been suggested to orient the sulfur toward C1 of the prenyl group (*6*). In the crystal structure of a FTase·isoprenoid·peptide ternary complex with the zinc removed, the bound peptide adopts a different conformation, and the sulfur of the cysteine residue is directed away from the zinc (*6*). While the ability of nonpeptidic thiol compounds to act as substrates for FTase could be attributed to the interaction with the zinc, the loss of additional interactions may contribute to the decreased binding affinity and catalytic efficiency of the thiol compounds.

The nonpeptidic thiol compounds are not efficient substrates for FTase. The single-turnover and steady-state rate constants are substantially lower, and the binding affinity is significantly reduced for the thiol compounds compared to the peptide GCVLS. The observed increases in the values of K_D, K_m, and $K_{1/2}$ demonstrate that zinc−thiolate coordination is not sufficient to achieve the high-affinity binding observed for peptide and protein substrates. In fact, the free energy of binding the thiol compounds to FTase·I_{ana} com-

plexes (~5 kcal/mol) is comparable to zinc−sulfur coordination energies observed in small-molecule zinc complexes [>4 kcal/mol (*67*)] and much smaller than the binding free energy of peptide substrates (10 kcal/mol for GCVLS). Therefore, other interactions between the peptide and the FTase·isoprenoid complex provide a significant portion of the binding energy. In addition to the decreased binding affinity, the free energy of the rate-limiting transition state relative to the FTase·FPP·RSH ground state ($\Delta\Delta G^{\ddagger}$) is increased 3−5 kcal/mol in comparison to the reaction with peptides: $\Delta\Delta G^{\ddagger} = \Delta G^{\ddagger}_{RSH} - \Delta G^{\ddagger}_{GCVLS} = RT \ln(k_{max}^{RSH}/k_{max}^{GCVLS})$.

Direct interactions between the Ca_1a_2X motif and residues in the active site of FTase play an important role in substrate specificity. Crystal structures of FTase·isoprenoid·peptide ternary complexes (*5*, *6*) confirmed the direct interaction of Arg202β with a_2 and Gln167α with X via hydrogen bonds. These interactions are even maintained in the absence of zinc (*6*), suggesting that they make significant contributions to the binding affinity of the peptide substrate. Additional stabilization could result from van der Waals contacts with FTase and the isoprenoid substrate and coordination of a water molecule at the base of the active site. The decreased binding affinities of the thiol compounds are consistent with loss of the direct and indirect interactions of a_2 and X with the enzyme. However, these interactions increase both binding and reactivity, either by enhancing the reactivity of the bound substrates or, more likely, by correctly positioning the substrates for optimal reactivity and magnesium affinity. These data suggest that, at a minimum, it is the combination of the zinc−sulfur coordination and the interaction of the a_2 and X residues of the Ca_1a_2X motif with the enzyme that determines the specificity and catalytic efficiency of FTase substrates.

Implications of Farnesylation of Nonpeptidic Thiols. The ability of FTase to use nonpeptidic thiol compounds as substrates could have important implications both in vivo and in vitro. Many cellular reactions require the presence of a reducing agent, usually glutathione. Glutathione levels in mammalian cells are typically 0.5−10 mM (*68*), suggesting that the intracellular concentration of glutathione could be comparable to the $K_{1/2}$ (10 mM) and K_m (5 mM) values measured here. In addition to glutathione, there are other intracellular thiol compounds, including cysteine and homocysteine, which are potential substrates for FTase. While it is possible that farnesyl-thiols could play an important cellular role, these compounds have not been observed in vivo, and the kinetic data presented here indicate that nonpeptidic thiols are not efficient substrates for FTase. Under k_{cat}/K_m conditions, farnesylation of peptides is catalyzed at a rate constant near the diffusion-controlled limit; peptide association is the rate-limiting step (*41*, *49*). However, for the thiol compounds, both substrate affinity and the farnesylation rate constant are decreased so that substrate binding becomes reversible and farnesylation is likely the rate-limiting step for turnover. This change in the kinetic mechanism further enhances the apparent specificity of FTase for peptides, suggesting that FTase activity in vivo may be tuned for farnesylation of protein substrates even in the presence of high concentrations of intracellular thiols.

Nonetheless, the data presented here suggest that thiol reducing agents should be used with caution when investigating the mechanism and specificity of protein prenyltransferases. Thiol compounds compete with peptides with respect to binding to the FTase·I_{ana} binary complex and, therefore, could compete with weakly binding peptides/proteins or inhibitors to mask important interactions. Additionally, the presence of many compounds, including DTT and TCEP, increases k_{cat} (K. E. Hightower and C. A. Fierke, unpublished data) due, presumably, to activation of product release (*52*), suggesting that the K_m and k_{cat} values of weakly binding substrates could be substantially altered. In addition, farnesyl-thiol products are not detected by traditional filter binding and biotin−avidin assays since the farnesyl-thiol will not be retained by the filter or the avidin. Finally, in single-turnover and pre-steady-state assays, where the enzyme is preincubated with FPP before addition of peptide, the presence of DTT in the buffer will result in the formation of farnesyl-DTT and a reduction in the endpoint value. Since the removal of reducing agents from most FTase assays is not possible, nonthiol reducing agents such as TCEP are a reasonable alternative to thiol reducing agents.

ACKNOWLEDGMENT

We thank Garrick Stewart, Kim Johnson, Calvin Wilder, and Dr. William Tschantz for performing the initial studies with these compounds, Dr. George Dubay for performing the mass spectrometry, and Dr. Chih-chin Huang, Dr. Rebecca Spence, and Dr. Matthew Saderholm for assistance and helpful discussions.

REFERENCES

1. Zhang, F. L., and Casey, P. J. (1996) *Annu. Rev. Biochem. 65*, 241−269.
2. Casey, P. J., and Seabra, M. C. (1996) *J. Biol. Chem. 271*, 5289−5292.
3. Sinensky, M. (2000) *Biochim. Biophys. Acta 1484*, 93−106.
4. Witter, D. J., and Poulter, C. D. (1996) *Biochemistry 35*, 10454−10463.
5. Strickland, C. L., Windsor, W. T., Syto, R., Wang, L., Bond, R., Wu, Z., Schwartz, J., Le, H. V., Beese, L. S., and Weber, P. C. (1998) *Biochemistry 37*, 16601−16611.
6. Long, S. B., Casey, P. J., and Beese, L. S. (2000) *Struct. Fold. Des. 8*, 209−222.
7. Long, S. B., Casey, P. J., and Beese, L. S. (1998) *Biochemistry 37*, 9612−9618.
8. Dunten, P., Kammlott, U., Crowther, R., Weber, D., Palmero, R., and Birktoft, J. (1998) *Biochemistry 37*, 7907−7912.
9. Park, H. W., Boduluri, S. R., Moomaw, J. F., Casey, P. J., and Beese, L. S. (1997) *Science 275*, 1800−1804.
10. Zhang, H., Seabra, M. C., and Deisenhofer, J. (2000) *Struct. Fold. Des. 8*, 241−251.
11. Huang, C., Casey, P. J., and Fierke, C. A. (1997) *J. Biol. Chem. 272*, 20−23.
12. Rozema, D. B., and Poulter, C. D. (1999) *Biochemistry 38*, 13138−13146.
13. Hightower, K. E., Huang, C., Casey, P. J., and Fierke, C. A. (1998) *Biochemistry 37*, 15555−15562.
14. Huang, C., Hightower, K. E., and Fierke, C. A. (2000) *Biochemistry 39*, 2593−2602.
15. Saderholm, M. J., Hightower, K. E., and Fierke, C. A. (2000) *Biochemistry 39*, 12389−12405.
16. Dolence, J. M., and Poulter, C. D. (1995) *Proc. Natl. Acad. Sci. U.S.A. 92*, 5008−5011.
17. Wu, Z., Demma, M., Strickland, C. L., Radisky, E. S., Poulter, C. D., Le, H. V., and Windsor, W. T. (1999) *Biochemistry 38*, 11239−11249.
18. Barbacid, M. (1987) *Annu. Rev. Biochem. 56*, 779−827.

19. Cox, A. D., and Der, C. J. (1997) *Biochim. Biophys. Acta 1333*, F51−F71.
20. Hancock, J. F., Magee, A. I., Childs, J. E., and Marshall, C. J. (1989) *Cell 57*, 1167−1177.
21. Schafer, W. R., Kim, R., Sterne, R., Thorner, J., Kim, S. H., and Rine, J. (1989) *Science 245*, 379−385.
22. Casey, P. J., Solski, P. A., Der, C. J., and Buss, J. E. (1989) *Proc. Natl. Acad. Sci. U.S.A. 86*, 8323−8327.
23. Qian, Y., Sebti, S. M., and Hamilton, A. D. (1997) *Biopolymers 43*, 25−41.
24. Gibbs, J. B., and Oliff, A. (1997) *Annu. Rev. Pharmacol. Toxicol. 37*, 143−166.
25. Oliff, A. (1999) *Biochim. Biophys. Acta 1423*, C19−C30.
26. Prendergast, G. C. (2000) *Curr. Opin. Cell Biol. 12*, 166−173.
27. Rowell, C. A., Kowalczyk, J. J., Lewis, M. D., and Garcia, A. M. (1997) *J. Biol. Chem. 272*, 14093−14097.
28. James, G. L., Goldstein, J. L., and Brown, M. S. (1995) *J. Biol. Chem. 270*, 6221−6226.
29. Whyte, D. B., Kirschmeier, P., Hockenberry, T. N., Nunez-Oliva, I., James, L., Catino, J. J., Bishop, W. R., and Pai, J.-K. (1997) *J. Biol. Chem. 272*, 14459−14464.
30. Zhang, F. L., Kirschmeier, P., Carr, D., James, L., Bond, R. W., Wang, L., Patton, R., Windsor, W. T., Syto, R., Zhang, R., and Bishop, W. R. (1997) *J. Biol. Chem. 272*, 10232−10239.
31. Parmryd, I., Shipton, C. A., Swiezewska, E., Andersson, B., and Dallner, G. (1996) *Eur. J. Biochem. 234*, 723−731.
32. Zimmerman, K. K., Scholten, J. D., Huang, C. C., Fierke, C. A., and Hupe, D. J. (1998) *Protein Expression Purif. 14*, 395−402.
33. Bradford, M. M. (1976) *Anal. Biochem. 72*, 248−254.
34. Ellman, G. L. (1959) *Arch. Biochem. Biophys. 82*, 70−77.
35. Riddles, P. W., Blakeley, R. L., and Zerner, B. (1979) *Anal. Biochem. 94*, 75−81.
36. Manne, V., Ricca, C. S., Brown, J. G., Tuomari, A. V., Yan, N., Patel, D., Schmidt, R., Lynch, M. J., Ciosek, C. P., Jr., Carboni, J. M., Robinson, S., Gordon, E. M., Barbacid, M., Seizinger, B. R., and Biller, S. A. (1995) *Drug Dev. Res. 34*, 121−137.
37. Naider, F. R., and Becker, J. M. (1997) *Biopolymers 43*, 3−14.
38. Xue, C.-B., Becker, J. M., and Naider, F. (1992) *Tetrahedron Lett. 33*, 1435−1438.
39. Goldstein, J. L., Brown, M. S., Stradley, S. J., Reiss, Y., and Gierasch, L. M. (1991) *J. Biol. Chem. 266*, 15575−15578.
40. Roskoski, R., Jr., and Ritchie, P. (1998) *Arch. Biochem. Biophys. 356*, 167−176.
41. Pompliano, D. L., Rands, E., Schaber, M. D., Mosser, S. D., Anthony, N. J., and Gibbs, J. B. (1992) *Biochemistry 31*, 3800−3807.
42. Reiss, Y., Goldstein, J. L., Seabra, M. C., Casey, P. J., and Brown, M. S. (1990) *Cell 62*, 81−88.
43. Reiss, Y., Stradley, S. J., Gierasch, L. M., Brown, M. S., and Goldstein, J. L. (1991) *Proc. Natl. Acad. Sci. U.S.A. 88*, 732−736.
44. Omer, C. A., Kral, A. M., Diehl, R. E., Prendergast, G. C., Powers, S., Allen, C. M., Gibbs, J. B., and Kohl, N. E. (1993) *Biochemistry 32*, 5167−5176.
45. Trueblood, C. E., Boyartchuk, V. L., and Rine, J. (1997) *Proc. Natl. Acad. Sci. U.S.A. 94*, 10774−10779.
46. Del Villar, K., Mitsuzawa, H., Yang, W., Sattler, I., and Tamanoi, F. (1997) *J. Biol. Chem. 272*, 680−687.
47. Del Villar, K., Urano, J., Guo, L., and Tamanoi, F. (1999) *J. Biol. Chem. 274*, 27010−27017.
48. Zhang, F. L., Fu, H. W., Casey, P. J., and Bishop, W. R. (1996) *Biochemistry 35*, 8166−8171.
49. Furfine, E. S., Leban, J. J., Landavazo, A., Moomaw, J. F., and Casey, P. J. (1995) *Biochemistry 34*, 6857−6862.
50. Mathis, J. R., and Poulter, C. D. (1997) *Biochemistry 36*, 6367−6376.
51. Spence, R. A., Hightower, K. E., Terry, K. L., Beese, L. S., Fierke, C. A., and Casey, P. J. (2000) *Biochemistry 39*, 13651−13659.
52. Tschantz, W. R., Furfine, E. S., and Casey, P. J. (1997) *J. Biol. Chem. 272*, 9989−9993.
53. Roberts, D. D., Lewis, S. D., Ballou, D. P., Olson, S. T., and Shafer, J. A. (1986) *Biochemistry 25*, 5595−5601.
54. Ogilvie, J. W., Tildon, J. T., and Strauch, B. S. (1964) *Biochemistry 3*, 754−758.
55. Wilson, J. M., Bayer, R. J., and Hupe, D. J. (1977) *J. Am. Chem. Soc. 99*, 7922−7926.
56. Whitesides, G. M., Lilburn, J. E., and Szajewski, R. P. (1977) *J. Org. Chem. 42*, 332−338.
57. Szajewski, R. P., and Whitesides, G. M. (1980) *J. Am. Chem. Soc. 102*, 2011−2026.
58. Bednar, R. A. (1990) *Biochemistry 29*, 3684−3690.
59. Dedon, P. C., and Goldberg, I. H. (1992) *Biochemistry 31*, 1909−1917.
60. Reiss, Y., Brown, M. S., and Goldstein, J. L. (1992) *J. Biol. Chem. 267*, 6403−6408.
61. Moomaw, J. F., and Casey, P. J. (1992) *J. Biol. Chem. 267*, 17438−17443.
62. Zhang, F. L., and Casey, P. J. (1996) *Biochem. J. 320*, 925−932.
63. Moores, S. L., Schaber, M. D., Mosser, S. D., Rands, E., O'Hara, M. B., Garsky, V. M., Marshall, M. S., Pompliano, D. L., and Gibbs, J. B. (1991) *J. Biol. Chem. 266*, 14603−14610.
64. Dolence, J. M., Cassidy, P. B., Mathis, J. R., and Poulter, C. D. (1995) *Biochemistry 34*, 16687−16694.
65. Rozema, D. B., Phillips, S. T., and Poulter, C. D. (1999) *Org. Lett. 1*, 815−817.
66. Chen, W. J., Moomaw, J. F., Overton, L., Kost, T. A., and Casey, P. J. (1993) *J. Biol. Chem. 268*, 9675−9680.
67. *NIST Critical Stability Constants of Metal Complexes Database 46* (1993) U.S. Department of Commerce.
68. Meister, A., and Anderson, M. E. (1983) *Annu. Rev. Biochem. 52*, 711−760.

BI002237D